Published in final edited form as:
Hypertension. 2009 February ; 53(2): 243–250. doi:10.1161/HYPERTENSIONAHA.108.118349.

TRPV1 gene deletion exacerbates inflammation and atypical cardiac remodeling after myocardial infarction

Wei Huang[1,2], **Jack Rubinstein**[1], **Alejandro R. Prieto**[1], **Loc Vinh Thang**[1], and **Donna H. Wang**[1,3,4]

1*Department of Medicine, Michigan State University*

2*Department of Cardiology, Chongqing Medical University, China*

3*Neuroscience Program, Michigan State University*

4*Cell and Molecular Biology Program, Michigan State University*

Abstract

The transient receptor potential vanilloid (TRPV1) channels expressed in sensory afferent fibers innervating the heart may be activated by proton or endovanilloids released during myocardial ischemia (MI), leading to angina. Although our previous *in vitro* data indicate that TRPV1 activation may preserve cardiac function after ischemia-reperfusion (I/R) injury, the underlying mechanisms are largely unknown. To test the hypothesis that TRPV1 modulates inflammatory and early remodeling processes to prevent cardiac functional deterioration after myocardial infarction, TRPV1-null mutant ($TRPV1^{-/-}$) and wild-type (WT) mice were subjected to left anterior descending coronary ligation or sham operation. The infarct size was greater in $TRPV1^{-/-}$ than in WT mice ($P < 0.001$) 3 days after MI, and the mortality rate was higher in $TRPV1^{-/-}$ than in WT mice ($P < 0.05$) 7 days after MI. The levels of plasma cardiac troponin I; cytokines including TNF-α, IL-1β, and IL-6; chemokines including MCP-1 and MIP-2; infiltration of inflammatory cells including neutrophil, macrophage, and myofibroblast; as well as collagen contents were greater in $TRPV1^{-/-}$ than in WT mice ($P < 0.05$) in the infarct area on day 3 and 7 after MI. Changes in left ventricular (LV) geometry led to increased end-systolic and -diastolic diameters and reduced contractile function in $TRPV1^{-/-}$ compared to WT mice. These data show that TRPV1 gene deletion results in excessive inflammation, disproportional LV remodeling, and deteriorated cardiac function after MI, indicating that TRPV1 may prevent infarct expansion and cardiac injury by inhibiting inflammation and abnormal tissue remodeling.

Keywords

transient receptor potential vanilloid subtype; myocardial infarction; inflammation; early remodeling, transgenic animal model

Introduction

The transient receptor potential vanilloid (TRPV1) receptor is a ligand—gated nonselective cation channel, primarily expressed in sensory nerves innervating the heart and blood vessels.[1-2] TRPV1 may function as a molecular integrator of multiple chemical and physical stimuli including protons, noxious heat, endovanilloids, and capsaicin (CAP).[3-4] Myocardial ischemia

Correspondence to: Donna H. Wang, MD., FAHA B316 Clinical Center, Michigan State University, East Lansing, MI 48824, 517-432-0797(p) 517-432-1326 (f) E-mail: Donna.Wang@ht.msu.edu.

Disclosures None.

causes release of protons and bradykinin, which may activate or sensitize TRPV1 expressed in cardiac sensory nerve terminals including unmyelinated C-fibers and thinly myelinated Aδ- fibers to cause angina.[5-6] Indeed, ischemic stimulation of cardiac afferent nerves has been shown to be mediated by activation of TRPV1.[1]

Using the isolated, perfused Langendorff heart preparation, we showed that TRPV1 protects the heart from post-ischemic reperfusion injury possibly via increasing substance P (SP) release from sensory nerve terminals.[7] Moreover, TRPV1 contributes to the beneficial effects of preconditioning (PC) of the heart against ischemia-reperfusion (I/R) injury via triggering the release of SP and/or calcitonin gene-related peptide (CGRP).[8] It has been shown that patients with pre-infarction angina have a better prognosis after acute infarction than those without, a phenomenon ascribed to ischemic PC.[9] However, it is unknown whether TRPV1, a molecular transmitter of pain, plays a protective role against myocardial infarction (MI) in vivo.

MI is accompanied by an inflammatory process, which is a prerequisite for healing and scar formation.[10] The degree of the inflammatory response is also a key determinant of the host's outcome.[11] The initial healing phase of the acute MI is characterized by mononuclear and fibroblast cell infiltration in the absence of polymorphonuclear leukocytes, and the later healing and remodeling processes are intertwined.[12] TRPV1 has been shown to play a protective role against endotoxin-induced inflammation and to facilitate wound healing in the cornea after injury.[13,14] TRPV1-induced neuropeptide release, including CGRP and SP, has also been shown to be involved in inflammation in a manner that they mediate distinct effects.[15,16] However, it is unknown whether TRPV1 plays a role in the cardiac inflammatory process after MI, and if so, how it affects cardiac healing and remodeling.

Patients with asymptomatic myocardial infarction show a higher mortality than those with symptoms.[17-18] Increased understanding of the role of cardiac TRPV1-positive sensory nerves in MI would help defining whether TRPV1 merely transmits a warning sign that a more severe attack is about to happen, or whether its activation protects the heart from MI injury by modulating cardiac inflammatory and healing processes. This study tests the hypothesis that TRPV1 regulates the inflammatory process and early remodeling to prevent cardiac functional deterioration after MI.

Methods

Animals and surgical procedures

Ten-week-old male TRPV1 knockout ($TRPV1^{-/-}$) or wild type (WT) mice (The Jackson Laboratory, Bar Harbor, ME) were subjected to either a proximally left anterior descending (LAD) ligation or a sham operation. Mice were anesthetized with pentobarbital (50mg/kg IP) and ventilated with room air using a MiniVent mouse ventilator (Hugo Sachs Elektronik, Germany). Incision was made in the fourth intercostal space to open the pericardium. MI was induced by a permanent LAD ligation with a 7-0 prolene suture (Ethicon),[19] and confirmed under a dissecting microscope (Olympus SZ30, Japan) by the discoloration of the ischemic area. Sham-operated animals underwent the same procedure except for LAD ligation. After surgery, mice were inspected at least three times daily to check for mortality and causes of death.[19] The surviving animals were randomly measured for cardiac function and subsequently killed on day 3 or 7 after surgery.

Risk area and infarct size

Evans blue dye (1%) was perfused into the aorta and coronary arteries and stained the non-ischemic area blue. Hearts were excised, sliced into 5 cross sections below the ligature, weighed, incubated in a 1% triphenyltetrazolium chloride (TTC) solution, and photographed

for infarct size calculation. The total LV area, risk area, and infarct area were determined using computer assisted software (NIH Image) and multiplied by the weight of the section. Three ratios were obtained: infarct area/area at risk (INF/AAR), infarct area/left ventricle (INF/LV), and area at risk/left ventricle (AAR/LV).

Immunohistochemical studies

The mouse hearts were dissected and fixed in 4% formaldehyde solution and embedded in paraffin. Sections (4-5 μm) were stained with the following antibodies: rat anti-mouse neutrophil antibody (AbD Serotec, Raleigh, NC), or rat anti-mouse macrophages antibody Mac-2 (Cedarlane, Burlington, Ontario, Canada). After rinsing, slides were incubated with either anti-neutrophil (1:75) or anti-Mac-2 (1:100), and incubated with a biotinylated rabbit anti-rat secondary antibody (1:100, Vector Laboratories, Burlingame, CA). For the staining of myofibroblasts, slides were incubated with primary mouse anti-myofibroblast cocktail (primary antibody, secondary antibody, normal mouse serum at a 1:200, 1:1000, 1:50 dilution, respectively, Vector Laboratories, Burlingame, CA), avidin alkaline phosphatase solution (KPL, Kierkegaard Perry Laboratories, Gaithersburg, MD), and then vector fast red (substrate kit #1, Vector Laboratories, Burlingame, CA). Masson's trichrome was performed according to a standard protocol.

Quantitative analysis

All quantitative analyses were performed by at least two independent investigators on blind specimens. Neutrophils, macrophages, and myofibroblasts were counted in stained sections. To determine the average cellular density (cells/mm^2), the stained cells in the peri-infarction zone were counted in ten different fields of 40X objective.

Determination of plasma cardiac troponin I

Before each mouse was sacrificed, they were injected with heparin and the blood was collected. The plasma concentration of cardiac troponin I (cTnI) was measured as an index of cardiac cellular damage by using the quantitative rapid assay kit (Life Diagnostics, West Chester, PA).

Determination of tissue cytokines and chemokines by ELISA assay

Protein levels of cytokines including tumor necrosis factor (TNF)-α, interleukin (IL)-6, and IL-1β, and chemokines including monocyte chemoattractant protein (MCP)-1 and macrophage inflammatory protein (MIP)-2 in the myocardium were determined using various ELISA kits (R&D System, Minneapolis, MN). Tissue samples of myocardium were homogenized in ice-cold PBS buffer containing protease inhibitor cocktail (50 mg wet wt/ml), and total proteins were extracted using NE-PER Cytoplasmic Extraction Reagents (Pierce, Rockford, IL). Total protein concentration (picograms per milligram total tissue protein) was determined using a Bio-Rad Protein Assay (Bio-Rad Laboratories, Hercules, CA).

Hydroxyproline assay for collagen content

The collagen content of the myocardial tissue was determined by the hydroxyproline assay.[20] Tissue was freeze-dried, weighed, homogenized in 0.1 mol/L NaCl and 5 mmol/L NaHCO3, washed 5 times with the same solution, and hydrolyzed in 0.5 ml 6N HCl. Samples were filtered and vacuum-dried, and then dissolved in distilled water. The hydroxyproline content was determined with a colorimetric assay by the protocol described in Chiariello et. al. using a 0.5-5μg hydroxyproline as a calibrated curve, and the data was expressed as micrograms collagen per milligram dry weight, assuming that collagen contains an average of 13.5% hydroxyproline.[20]

Transthoracic echocardiography

Three or seven days after MI, the mice were re-anesthetized with pentobarbital (50mg/kg IP) and placed on a heating pad. Echocardiography was performed using a GE Vivid 7/Vingmed ultrasound machine (General Electric, Milwaukee, WI) with a 10 MHz transducer applied parasternally to the shaved chest wall. The following parameters were measured as indicators of function and remodeling: left ventricular internal diameter in diastole (LVIDd), left ventricular internal diameter in systole (LVIDs), posterior wall thickness (PWth), and the ejection fraction was directly calculated with integrated software using the Teicholz formula derived from a fractional shortening measurement (LVIDd-LVIDs/LVIDd * 100).

Statistical analysis

All values were expressed as mean ± SE. The difference among groups for the percentages of survival rate and the area at risk were analyzed using one-way ANOVA follow by Bonferroni adjustment for multiple comparison. The data from the echocardiography studies, the plasma cardiac troponin I, the levels of inflammatory cells, cytokine, chemokine, and collagen content were analyzed by two-way ANOVA follow by Bonferroni adjustment for multiple comparisons. Differences were considered statistically significant at $P<0.05$.

Results

Lower survival rate in TPRV1$^{-/-}$ mice after MI

All sham-operated mice in both strains survived until the end of the experimental period. In contrast, as shown in Figure 1, TPRV1$^{-/-}$ mice had a significantly lower survival rate after MI compared to that of WT mice. The most frequent cause of death in both TRPV1$^{-/-}$ and WT mice was LV rupture.

Increased infarct size in TRPV1$^{-/-}$ mice after MI

Figure 2 shows that LAD ligation produced a larger infarct size in the LV wall in TRPV1$^{-/-}$ mice compared to WT mice (Figure 2A). Quantitative analyses showed that the infarct size was greater in TRPV1$^{-/-}$ mice compared to WT mice (Figure 2B).

Further elevated plasma cardiac troponin I levels in TRPV1$^{-/-}$ mice after MI

Figure 3 shows that plasma cTnI levels were increased 3 days after MI in both TRPV1$^{-/-}$ and WT mice, with a higher level in the former than latter. On day 7 after MI, plasma cTnI levels remained elevated in TRPV1$^{-/-}$ but not WT mice.

Augmented inflammation infiltration in TRPV1$^{-/-}$ mice after MI

Figure 4 shows that, on day 3 after MI, both TRPV1$^{-/-}$ and WT mouse hearts exhibited infiltration of peri-infarct myocardium with neutrophils, and showed extensive replacement of dead cardiomyocytes with granulation tissues. TRPV1$^{-/-}$ hearts, compared to WT hearts, showed enhanced elevation of neutrophil density in the peri-infarct myocardium on day 3 and day 7 after MI. Attenuated infiltration of neutrophil on day 7 compared to day 3 after MI in both TRPV1$^{-/-}$ and WT hearts indicated clearance of the neutrophilic infiltrate by day 7.

Figure 5 shows macrophages infiltration of peri-infarct myocardium on days 3 and 7 after MI in both TRPV1$^{-/-}$ and WT hearts. Macrophage density in the peri-infarct myocardium 3 or 7 days after MI was increased in both TRPV1$^{-/-}$ and WT hearts, with the former mice having even greater elevation. In contrast to clearance of neutrophilic infiltrate on day 7, macrophage density was higher in both strains on day 7 compared to day 3 after MI. Enhanced inflammatory cell infiltration observed on days 3 or 7 after MI in TRPV1$^{-/-}$ mice suggests that TRPV1

deficiency might prolong the time course of resolution of the inflammatory process in healing infarct.

Figure 6 shows that cardiac infarcts 3 or 7 days after MI were infiltrated with myofibroblasts, characterized with spindle-shaped α-smooth muscle actin-expressing cells. TRPV1$^{-/-}$ hearts, compared to WT hearts, showed significantly increased myofibroblast density in the peri-infarct myocardium. Similarly to changes in macrophage density, myofibroblast density was higher in both strains on day 7 compared to day 3 after MI.

Augmented expression of inflammatory cytokines and chemokines in TRPV1$^{-/-}$ mice after MI

Figure 7 shows up-regulated cytokines including TNF-α, IL-1β, and IL-6, and Figure 8 shows elevated chemokines including MCP-1 and MIP-2 in the infarct regions on day 3 or 7 post-MI in TPRV1$^{-/-}$ and WT mice. The increases in cytokines and chemokines at both time points were significantly higher in TPRV1$^{-/-}$ than in WT mice, with the exception of no significant difference in MIP-2 between TPRV1$^{-/-}$ and WT mice on day 7 post-MI (Figure 8B). Cytokine and chemokine levels were attenuated on day 7 compared to day 3 after MI in both TRPV1$^{-/-}$ and WT hearts.

Enhanced collagen deposition in TRPV1$^{-/-}$ mice after MI

Figure 9 shows that, in both strains, collagen continued to accumulate at the site of infarction from day 3 to day 7 after MI. In the infarct zone itself, the collagen deposition was not different between the 2 strains. However, conspicuously increased collagen deposition was observed in peri-infarct sites in TRPV1$^{-/-}$ compared to WT mice (Figure 9A). Quantitative analysis also showed increased collagen contents in the peri-infarct region in TRPV1$^{-/-}$ compared to WT mice (Figure 9B), and the increases were enhanced on day 7 compared to day 3 post-MI in both strains.

Enhanced remodeling and deterioration of cardiac function in TRPV1$^{-/-}$ mice after MI

As shown in Table 1, there was no significant difference in body weight or heart rate on days 3 or 7 post-MI among 4 groups. An increase in LVID and a decrease in EF were evident on day 3 in both TRPV1$^{-/-}$ and WT MI groups compared to sham-operated animals, and they were worse in TRPV1$^{-/-}$ compared to WT in MI groups. Enhanced thickening of PWthd/PWths and a further increase in LVID were observed in TRPV1$^{-/-}$ compared to WT mice 7 days after MI, suggesting of exaggerated progression of remodeling and LV dilation in TRPV1$^{-/-}$ MI mice. These geometric changes were accompanied by a further functional deterioration in TRPV1$^{-/-}$-MI mice as indicated by progressive decreases in EF compared to the corresponding WT MI mice on day 7.

Discussion

We demonstrate for the first time that TRPV1 deficiency results in increased mortality, aggravated inflammatory response, enhanced cardiac fibrosis, exaggerated progression of LV remodeling, and deteriorated cardiac function after acute MI. The molecular basis underlying deteriorated cardiac functional and structural changes post-MI may involve intensified inflammatory cell infiltration, cytokine/chemokine production/release, and collagen deposition in TRPV1$^{-/-}$ mice . A cautionary note entails that the mechanisms involved in the post-MI inflammation and myocardial remodeling may include complex pathways other than the TRPV1-mediated process.[6, 9, 10], The data generated from global knockout mice may need to be interpreted with the caution that compromised systemic changes may occur, which may affect the disease process or outcome.

Two essential prognostic factors that assess MI recovery deal with the infarct size and LV remodeling. We found that the increase in infarct size in TRPV1$^{-/-}$ mice was accompanied by a higher mortality rate due to LV ruptures and/or congestive heart failure. Cardiac rupture is an acute fatal complication in the early days after MI, which is primarily associated with matrix metalloproteinase (MMP)-induced collagen degradation.[21] TRPV1 deletion may induce an earlier degradation of existing collagen, contributing to cardiac rupture. Given that collagen contents in the heart are the results of a dynamic balance between collagen synthesis and degradation,[21,22] we are not certain whether increased collagen contents on days 3 and 7 after MI in TRPV1$^{-/-}$ mice were a compensatory response to an accelerated degradation of collagen or a direct stimulating effect on collagen synthesis.

Consistent with the increased infarct size, TRPV1$^{-/-}$ mice also presented a higher plasma cTnI level up to day 7 after MI while it returned to the baseline in WT mice. In comparison to higher mammals, mice show a more rapid and transient response with conversion of necrotic myocardium to granulation tissues mostly completed within a week.[23, 24] Our results of the plasma cTnI level in WT mice are consistent with these reports, whereas it takes more than a week after MI for the plasma cTnI level returning to normal in human.[24]

Enlarged infarct size induced by TRPV1 deficiency may involve several cell death pathways. It has been shown that TRPV1 activation inhibits TNF-dependent activation of nuclear factor-κB (NF- κB).[25] NF- κB is an ubiquitously expressed dimeric transcription factor involved in a number of biological processes including inflammation, cell adhesion, and cell survival[26] Activation of NF- κB increases tissue injury after acute MI.[27] One possible mechanism contributing to enlarged infarct size is that TRPV1 deletion would remove the inhibition of NF-κB activation, resulting in NF-κB-induced enhancement of inflammatory response and subsequent myocardial damage. Indeed, several cytokines including TNF-α, IL-1β, IL-6 and chemokine such as MCP-1 have a κB-binding domain in their promoter sites and expression of these molecules is governed by NF-κB.[28]

The consequences of inflammatory processes after MI can be favorable or harmful, with the former leading to healing and restoration of function and the latter leading to acute cardiac rupture or chronic cardiac dilatation due to excess necrosis and apoptosis.[11] We observed remarkable neutrophil and macrophage infiltration into the peri-infarct area in TRPV1$^{-/-}$ and WT mice after MI. The peri-infarct area or infarct border zone is the site of interface between surviving cardiomyocytes and newly formed granulation tissues, has a unique extracellular matrix composition, and serves as a barrier for expansion of the inflammatory/fibrotic response into the non-infarct areas.[29] While TRPV1$^{-/-}$ mice showed no evidence of spontaneous cardiac inflammation, an intense inflammatory response in the peri-infarct area is triggered after MI in this strain.

Ablation of TRPV1 might affect neutrophil migration given that TRPV1 is expressed in human and murine neutrophils and its activation leads to calcium influx. [30-31] Alternatively, excessive production of proinflammatory cytokines/chemokines seen in TRPV1$^{-/-}$ mice is likely to contribute to intensified infiltration of the non-infarct area with neutrophils, macrophages, and myofibroblasts,[32-33] resulting in expansion of granulation tissue formation, excessive collagen deposition, and disproportional remodeling in TRPV1$^{-/-}$ mice.[34,35] Unsuppressed inflammatory response after granulation tissue formation and unlimited expansion of fibrosis to the non-infarct myocardium would prevent the switch from inflammatory to healing processes, leading to persistent tissue damage.[29,36]

It seems paradoxical that TRPV1 deficient mice displayed both excessive collagen deposition in the posterior wall and enlarged LV after MI when considering that the scar is relatively non-distensible and resistant to deformation.[37] The process of ventricular enlargement can be

influenced by at least three interdependent factors, i.e. infarct size, degree of healing, and ventricular wall stresses.[38] Given that the infarct area was mostly in the anterior wall, the posterior wall may have compensated with increase thickness in the TRPV1$^{-/-}$ hearts, and may contribute to the ventricular enlargement seen. Moreover, in light of the fact that the infarct region is particularly vulnerable to distorted forces, the presence of an enlarged LV as early as 3 days after MI may exacerbate LV expansion as noted by increase in the end-systolic diameter (a powerful predictor of death).[38]

The extent of LV dilation after MI is an important determinant of risk for major adverse cardiovascular events including ventricular arrhythmias, heart failure, and death.[39] Patients with more extensive LV remodeling are at greater risks for cardiovascular fatalities, including sudden death attributable to ventricular arrhythmias due to slower pulse propagation velocities through myocardium partially replaced by fibrosis where anisotropic reentry occurs.[40] Furthermore, increased collagen deposition changes ventricular compliance, resulting in increased stiffness and altered LV performance, which contributes to increased incidence of congestive heart failure, aneurysm formation, and mortality.[21] Thus, uncontrolled cardiac remodeling observed in TRPV1$^{-/-}$ mice would predict a worse prognosis after MI.

Clinical perspective

A higher mortality rate occurs among silent MI, particularly in aging and diabetic populations[17-18] where defects in TRPV1-positive sensory nerve function are known.[41,42] In contrast, patients with pre-infarction angina have a better prognosis after MI than those without, and TRPV1 has been implicated in mediating the pain sensation of angina and the beneficial effect of preconditioning due to pre-infarct ischemia. However, direct evidence of TRPV1 playing a key role in inflammation and healing after MI is lacking. This study indicates that TRPV1 may play a protective role in post-infarction healing possibly via anti-inflammation mechanism and may serve as a new target for improving clinical outcomes after acute MI.

Acknowledgements

Sources of Funding This work was supported in part by National Institutes of Health (grants HL-57853, HL-73287, and DK67620).

References

1. Pan HL, Chen SR. Sensing tissue ischemia: another new function for capsaicin receptors? Circulation 2004;110:1826–1831. [PubMed: 15364816]
2. Szalasi A, Blumberg PM. Vanilloid (Capsaicin) receptors and mechanisms. Pharmacol Rev 1999;51:159–212. [PubMed: 10353985]
3. Caterina MJ, Schumacher MA, Tominaga M, Rosen TA, Levine JD, Julius D. The capsaicin receptor: a heat-activated ion channel in the pain pathway. Nature 1997;389:816–824. [PubMed: 9349813]
4. Caterina MJ, Leffler A, Malmberg AB, Martin WJ, Trafton J, Petersen-Zeitz KR, Koltzenburg M, Basbaum AI, Julius D. Impaired nociception and pain sensation in mice lacking the capsaicin receptor. Science 2000;288:306–313. [PubMed: 10764638]
5. Zahner MR, Li DP, Chen SR, Pan HL. Cardiac vanilloid receptor 1-expressing afferent nerves and their role in the cardiogenic sympathetic reflex in rats. J Physiol 2003;551:515–2314. [PubMed: 12829722]
6. Bolli R, Latif A. No pain, no gain: the useful function of angina. Circulation 2005;112:3541–3543. [PubMed: 16330693]
7. Wang L, Wang DH. TRPV1 gene knockout impairs postischemic recovery in isolated perfused heart in mice. Circulation 2005;112:3617–3623. [PubMed: 16314376]

8. Zhong B, Wang DH. TRPV1 gene knockout impairs preconditioning protection against myocardial injury in isolated perfused hearts in mice. Am J Physiol Heart Circ Physiol 2007;293:H1791–H1798. [PubMed: 17586621]

9. Yellon DM, Dana A. The preconditioning phenomenon: a tool for the scientistor a clinical reality? Cir Res 2000;87:543–550.

10. Frangogiannis NG, Smith CW, Entman ML. The inflammatory response in myocardial infarction. Cardiovasc Res 2002;53:31–47. [PubMed: 11744011]

11. Nian M, Lee P, Khaper N, Liu P. Inflammatory cytokines and postmyocardial infarction remodeling. Circ Res 2004;94:1543–1553. [PubMed: 15217919]

12. Solomon SD, Pfeffer MA. Renin-angiotensin system and cardiac rupture after myocardial infarction. Circulation 2002;106:2167–2169. [PubMed: 12390941]

13. Clark N, Keeble J, Fernandes ES, Starr A, Liang L, Sugden D, de Winter P, Brain SD. The transient receptor potential vanilloid 1 (TRPV1) receptor protects against the onset of sepsis after endotoxin. FASEB J 2007;21:3747–3755. [PubMed: 17601984]

14. Murata Y, Masuko S. Peripheral and central distribution of TRPV1, substance P and CGRP of rat corneal neurons. Brain Res 2006;1085:87–94. [PubMed: 16564032]

15. Levite M, Cahalon L, Hershkoviz R, Steinman L, Lider O. Neuropeptides, via specific receptors, regulate T cell adhesion to fibronectin. J Immunol 1998;160:993–1000. [PubMed: 9551939]

16. Helyes Z, Elekes K, Németh J, Pozsgai G, Sándor K, Kereskai L, Börzsei R, Pintér E, Szabó A, Szolcsányi J. Role of transient receptor potential vanilloid 1 receptors in endotoxin-induced airway inflammation in the mouse. Am J Physiol Lung Cell Mol Physiol 2007;292:L1173–L1181. [PubMed: 17237150]

17. Tresch DD. Management of the older patient with acute myocardial infarction: difference in clinical presentations between older and younger patients. J Am Geriatr Soc 1998;46:1157–1162. [PubMed: 9736113]

18. Rutter MK, Wahid ST, McComb JM, Marshall SM. Significance of silent ischemia and microalbuminuria in predicting coronary events in asymptomatic patients with type 2 diabetes. J Am Coll Cardiol 2002;40:56–61. [PubMed: 12103256]

19. Gao XM, Dart AM, Dewar E, Jennings G, Du XJ. Serial echocardiographic assessment of left ventricular dimensions and functionh after myocardial infarction in mice. Cardiovasc Res 2000;45:330–338. [PubMed: 10728353]

20. Peng H, Carretero OA, Alfie ME, Masura JA, Rhaleb NE. Effects of angiotensin-converting enzyme inhibitor and angiotensin type 1 receptor antagonist in deoxycorticosterone acetate-salt hypertensive mice lacking Ren-2 gene. Hypertension 2001;37:974–980. [PubMed: 11244026]

21. Sun M, Dawood F, Wen WH, Chen M, Dixon I, Kirshenbaum LA, Liu PP. Excessive tumor necrosis factor activation after infarction contributes to susceptibility of myocardial rupture and left ventricular dysfunction. Circulation 2004;110:3221–3228. [PubMed: 15533863]

22. Dewald O, Ren G, Duerr GD, Zoerlein M, Klemm C, Gersch C, Tincey S, Michael LH, Entman ML, Frangogiannis NG. Of mice and dogs: species-specific differences in the inflammatory response following myocardial infarction. Am J Pathol 2004;164:665–677. [PubMed: 14742270]

23. Virag JI, Murry CE. Myofibroblast and endothelial cell proliferation during murine myocardial infarct repair. Am J Pathol 2003;163:2433–2440. [PubMed: 14633615]

24. Cummins B, Auckland ML, Cummins P. Cardiac-specific troponin-I radioimmunoassay in the diagnosis of acute myocardial infarction. Am Heart J 1987;113:1333–1344. [PubMed: 3591601]

25. Singh S, Natarajan K. Capsaicin (8-methyl-N-vanillyl-6-nonenamide) is a potent inhibitor of nuclear transcription factor-kappa B activation by diverse agents. J Immunol 1996;157:4412–4420. [PubMed: 8906816]

26. Baeuerle PA, Baltimore D. NF-kappa B: ten years after. Cell 1996;87:13–20. [PubMed: 8858144]

27. Misra A, Haudek SB, Knuefermann P, Vallejo JG, Chen ZJ, Michael LH, Sivasubramanian N, Olson EN, Entman ML, Mann DL. Nuclear factor-kappaB protects the adult cardiac myocyte against ischemia-induced apoptosis in a murine model of acute myocardial infarction. Circulation 2003;108:3075–3078. [PubMed: 14676146]

28. Li HL, Zhuo ML, Wang D, Wang AB, Cai H, Sun LH, Yang Q, Huang Y, Wei YS, Liu PP, Liu DP, Liang CC. Targeted cardiac overexpression of A20 improves left ventricular performance and

reduces compensatory hypertrophy after myocardial infarction. Circulation 2007;115:1885–1894. [PubMed: 17389268]

29. Frangogiannis NG, Ren G, Dewald O, Zymek P, Haudek S, Koerting A, Winkelmann K, Michael LH, Lawler J, Entman ML. Critical role of endogenous thrombospondin-1 in preventing expansion of healing myocardial infarcts. Circulation 2005;111:2935–2942. [PubMed: 15927970]
30. Heiner I, Eisfeld J, Lückhoff A. Role and regulation of TRP channels in neutrophil granulocytes. Cell Calcium 2003;33:533–540. [PubMed: 12765698]
31. Waning J, Vriens J, Owsianik G, Stüwe L, Mally S, Fabian A, Frippiat C, Nilius B, Schwab A. A novel function of capsaicin-sensitive TRPV1 channels: involvement in cell migration. Cell Calcium 2007;42:17–25. [PubMed: 17184838]
32. Hensellek S, Brell P, Schaible HG, Bräuer R, von Banchet G Segond. The cytokine TNFalpha increases the proportion of DRG neurones expressing the TRPV1 receptor via the TNFR1 receptor and ERK activation. Mol Cell Neurosci 2007;36:381–391. [PubMed: 17851089]
33. Zhang N, Inan S, Cowan A, Sun R, Wang JM, Rogers TJ, Caterina M, Oppenheim JJ. A proinflammatory chemokine, CCL3, sensitizes the heat- and capsaicin-gated ion channel TRPV1. Proc Natl Acad Sci U S A 2005;102:4536–4541. [PubMed: 15764707]
34. van Amerongen MJ, Harmsen MC, van Rooijen N, Petersen AH, van Luyn MJ. Macrophage depletion impairs wound healing and increases left ventricular remodeling after myocardial injury in mice. Am J Pathol 2007;170:818–829. [PubMed: 17322368]
35. Szabó A, Czirják L, Sándor Z, Helyes Z, László T, Elekes K, Czömpöly T, Starr A, Brain S, Szolcsányi J, Pintér E. Investigation of sensory neurogenic components in a bleomycin-induced scleroderma model using transient receptor potential vanilloid 1 receptor- and calcitonin gene-related peptide-knockout mice. Arthritis Rheum 2008;58:292–230. [PubMed: 18163477]
36. Nathan C. Points of control in inflammation. Nature 2002;420:846–852. [PubMed: 12490957]
37. Parmley WW, Chuck L, Kivowitz C, Matloff JM, Swan HJ. In vitro length-tension relations of human ventricular aneurysms. Relation of stiffness to mechanical disadvantage. Am J Cardiol 1973;32:889–894. [PubMed: 4271258]
38. Pfeffer MA, Braunwald E. Ventricular remodeling after myocardial infarction. Experimental observations and clinical implications. Circulation 1990;81(4):1161–1172. [PubMed: 2138525]
39. Sutton, M John; Pfeffer, MA.; Moye, L.; Plappert, T.; Rouleau, JL.; Lamas, G.; Rouleau, J.; Parker, JO.; Arnold, MO.; Sussex, B.; Braunwald, E. Cardiovascular death and left ventricular remodeling two years after myocardial infarction: baseline predictors and impact of long-term use of captopril: information from the Survival and Ventricular Enlargement (SAVE) trial. Circulation 1997;96:3294–3299. [PubMed: 9396419]
40. Sutton, M John; Lee, D.; Rouleau, JL.; Goldman, S.; Plappert, T.; Braunwald, E.; Pfeffer, MA. Left ventricular remodeling and ventricular arrhythmias after myocardial infarction. Circulation 2003;107:2577–2582. [PubMed: 12732606]
41. Wang S, Davis BM, Zwick M, Waxman SG, Albers KM. Reduced thermal sensitivity and Nav1.8 and TRPV1 channel expression in sensory neurons of aged mice. Neurobiol Aging 2006;27:895–903. [PubMed: 15979214]
42. Bour-Jordan, Bluestone JA. Sensory neurons link the nervous system and autoimmune diabetes. Cell 2006;127:1097–1099. [PubMed: 17174888]

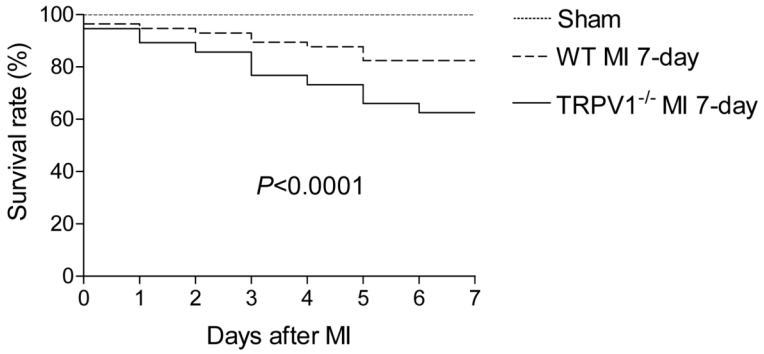

Figure 1.

The survival rate of TRPV1$^{-/-}$ and WT mice after myocardial infarction (MI). Survival curves were plotted for both TRPV1$^{-/-}$ mice (n = 56) and WT (n = 56) mice as determined with the Kaplan-Meier method. Log-rank $P<0.0001$.

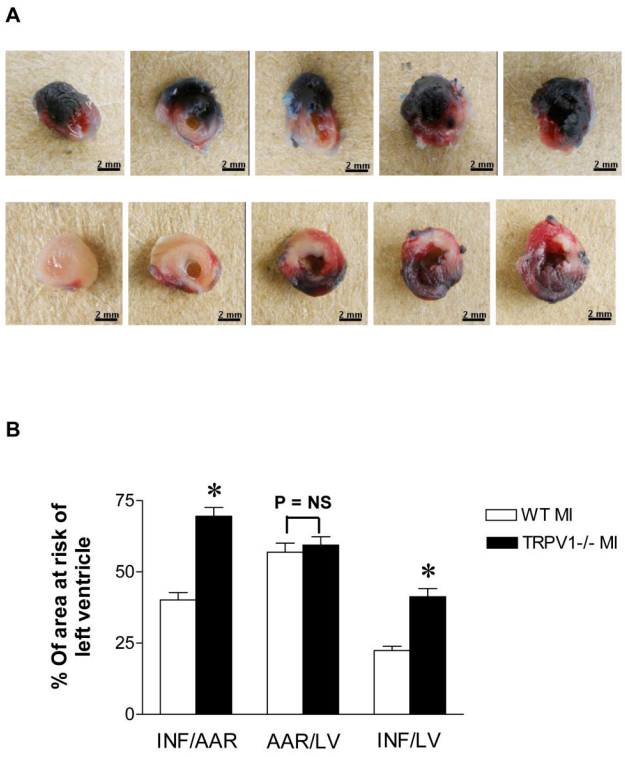

Figure 2.

A, Evan blue/TTC staining in WT and TRPV1$^{-/-}$ mice : Left ventricle views of WT (upper panel) and TRPV1$^{-/-}$ (lower panel) mice 3 days after MI. Pale area: infarct myocardium; TTC-stained area (red): ischemic but viable myocardium (area at risk); Evans blue-stained areas (blue): non-ischemic area. B, Infarct size in WT vs. TRPV1$^{-/-}$ mice 3 days after myocardial infarction. Infarction (INF) per area at risk (AAR) or left ventricle (LV) and AAR per LV. n=8-9, *P< 0.05.

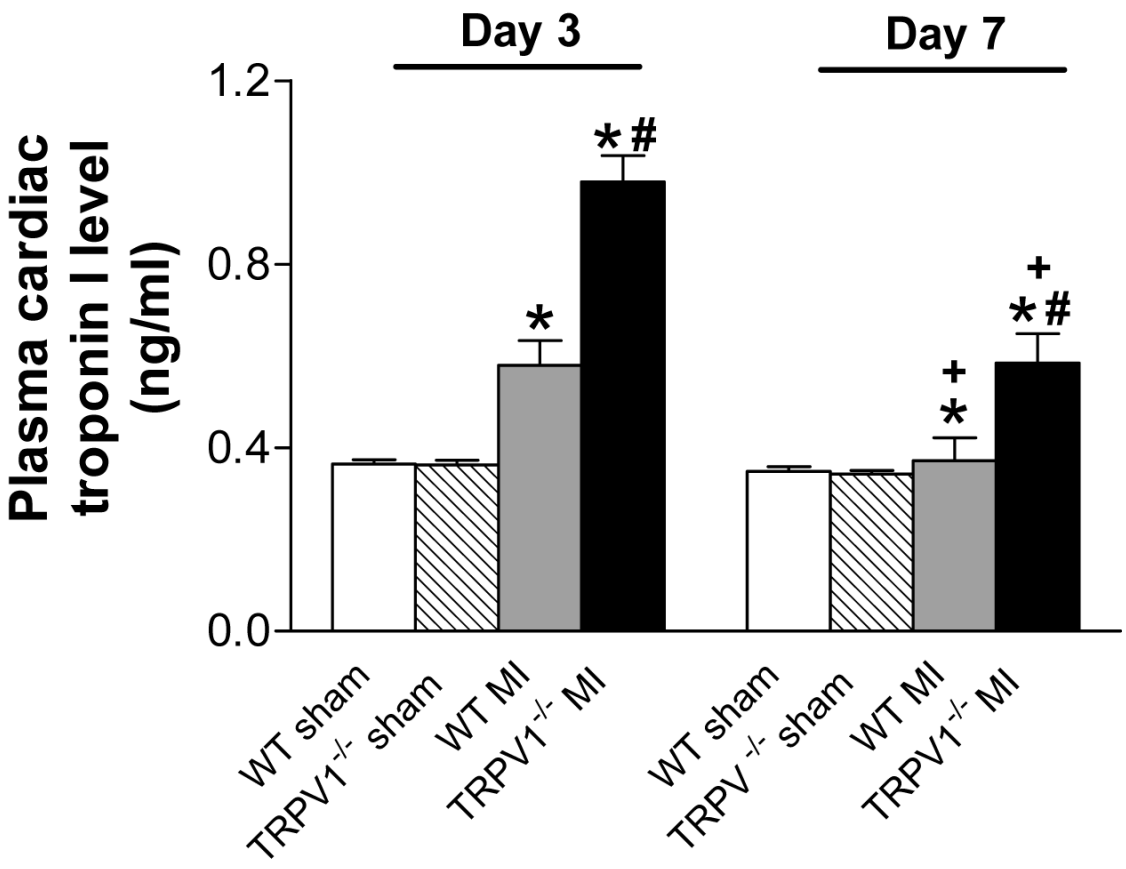

Figure 3.
Plasma cardiac troponion I levels after myocardial infarction (MI). n=8-9, **P*<0.05 vs. corresponding sham; †*P*<0.05 vs. WT at the same time point; ‡*P*<0.05 vs. corresponding day 3.

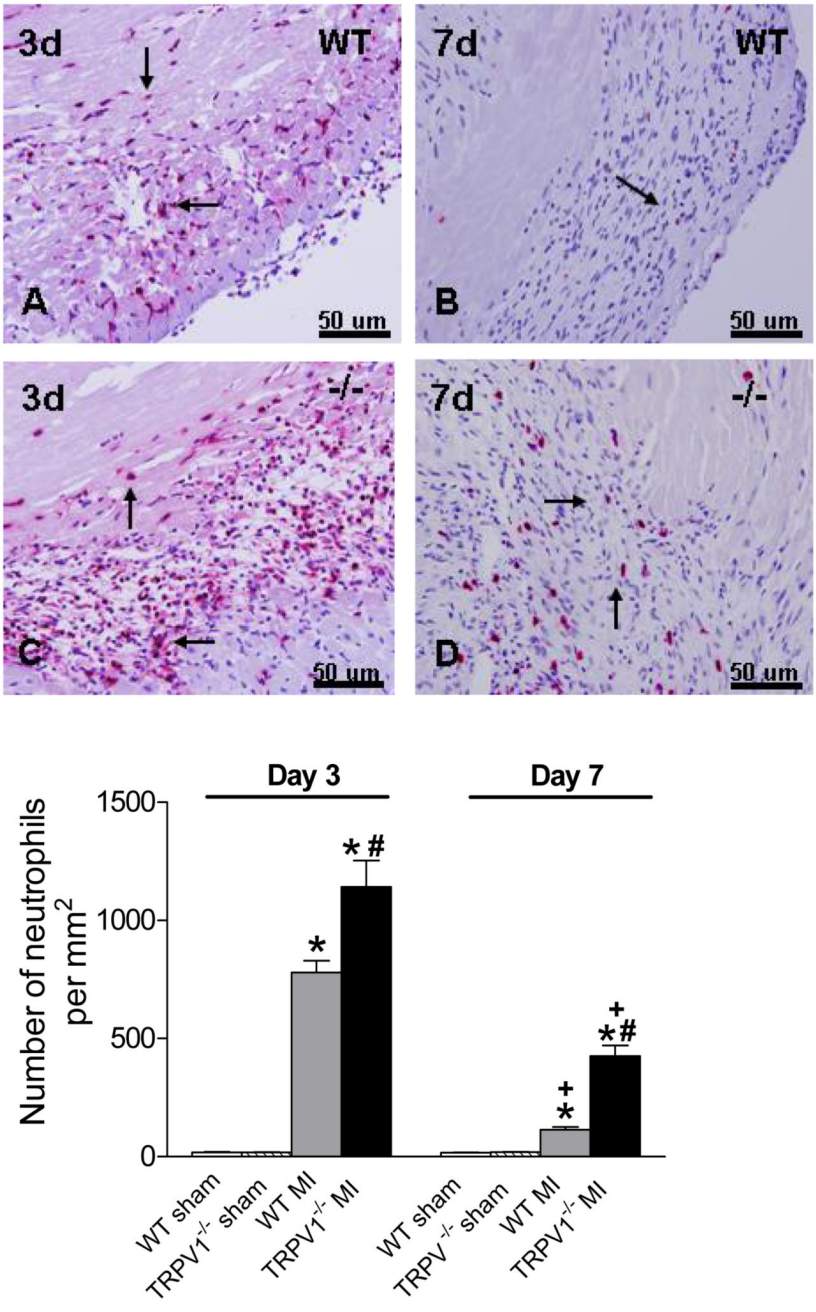

Figure 4.

Neutrophil infiltration in the peri-infarct zone. Upper panel: Netrophils per high-power filed in the border zone (x400, red-stained cells, arrow). Lower panel: Number of neutrophils per square millimeter. N=8-9, **P*<0.01 vs corresponding WT; †*P*<0.05 vs. WT at the same time point; ‡*P*<0.05 vs. corresponding day 3.

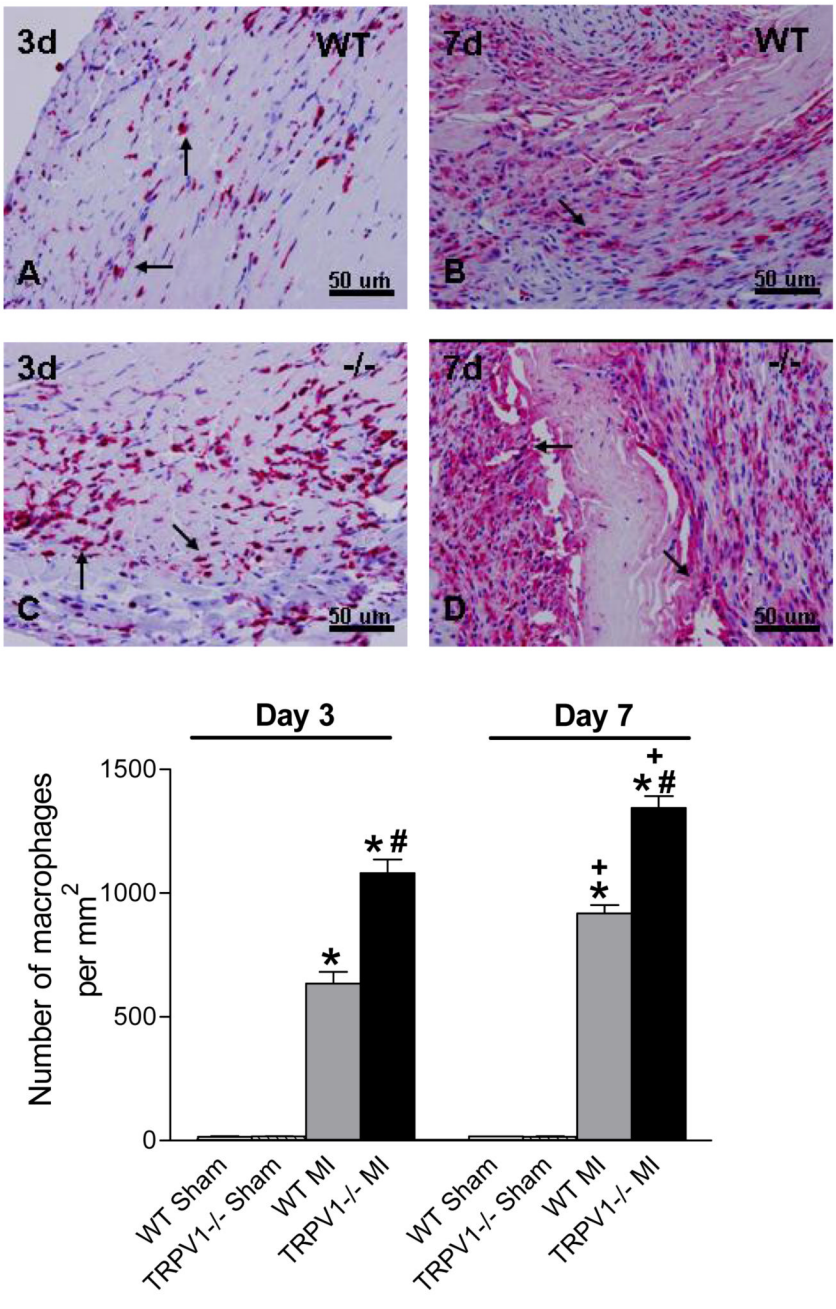

Figure 5.

Macrophage infiltration in the peri-infarct zone. Upper panel: Macrophage per high-power filed in the border zone (x 400, red-stained cells, arrow). Lower panel: Number of macrophages per square millimeter. N=8-9, **P*<0.05 vs corresponding WT; †*P*<0.05 vs. WT at the same time point; ‡*P*<0.05 vs. corresponding day 3.

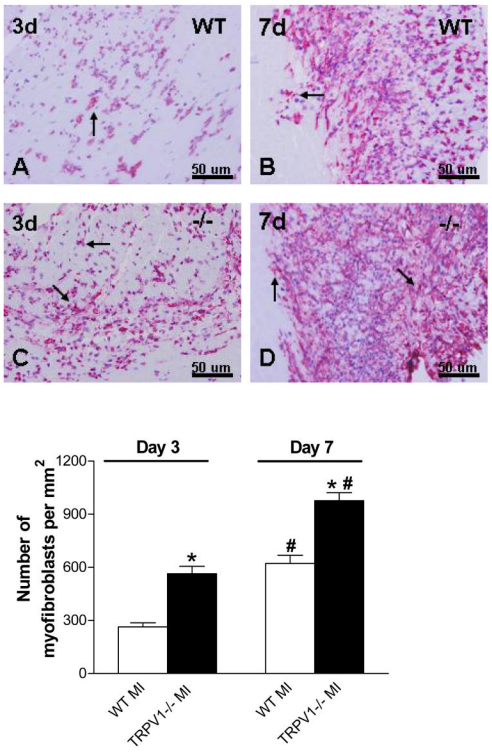

Figure 6.

Myofibroblasts infiltration in the peri-infarct zone. Upper panel: Myofibroblast per high-power filed in the border zone (x 400, red-stained cells, arrow); Lower portion: Number of myofibroblasts per square millimeter. N=8-9, **P*<0.01 vs corresponding WT; †*P*<0.01 vs corresponding day 3.

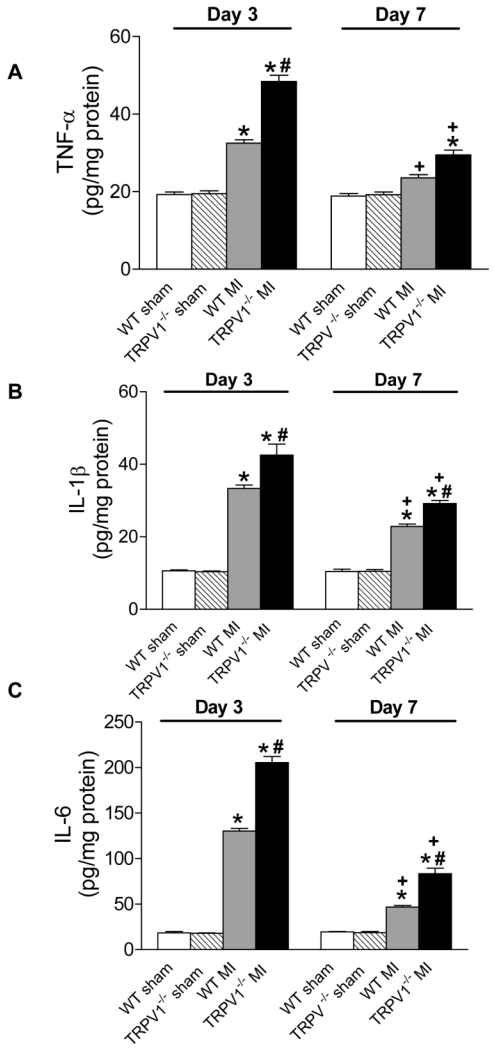

Figure 7.

Cytokine expression in the infarcted zone. TNF-α (A), IL-1β (B), and IL-6 (C) expression analyzed by ELISA. Results are expressed as mean ± SEM. n=8. **P*<0.05 vs corresponding sham; †*P*<0.01 vs corresponding WT; ‡*P* <0.01 vs corresponding day 3.

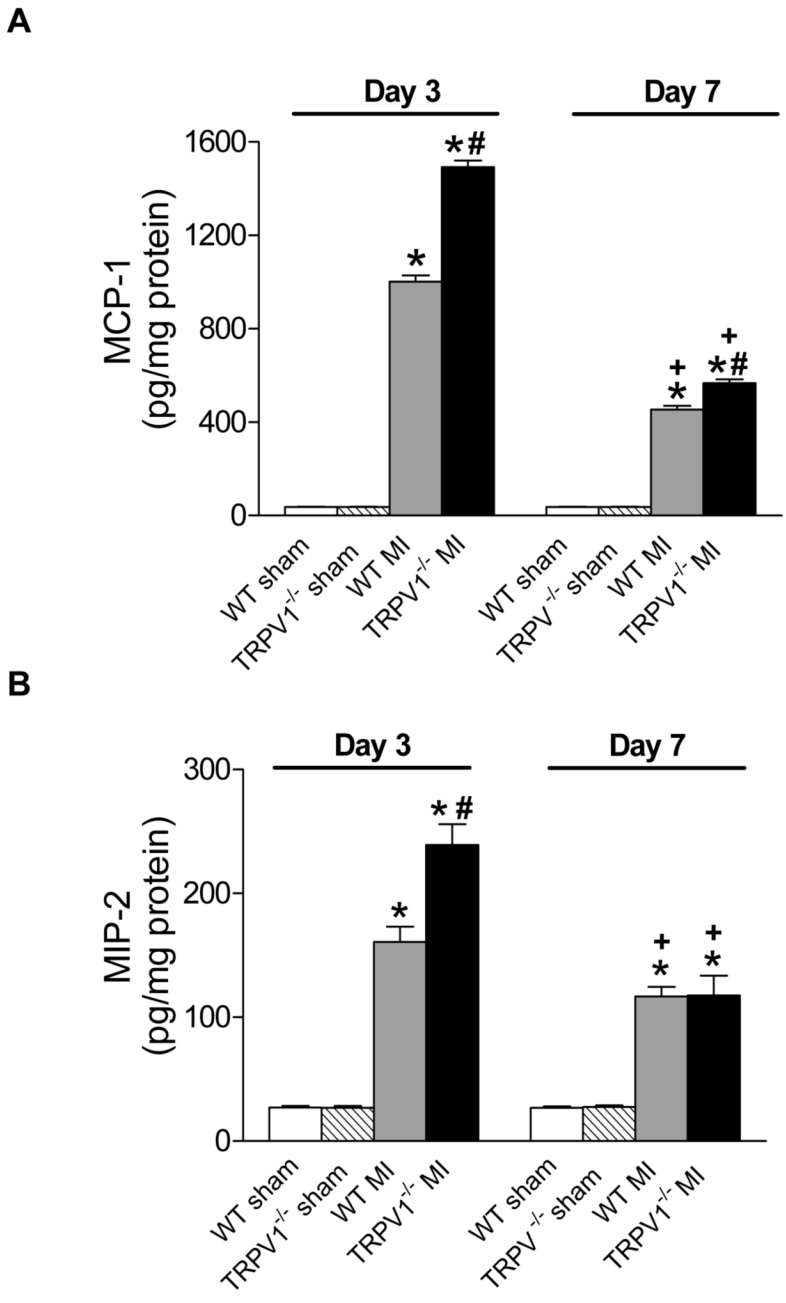

Figure 8.

Chemokines expression in infarcted zone. MCP-1 (A) and MIP-2 (B) expression analyzed by ELISA. Results are expressed as mean ± SEM. n=8. **P*<0.05 vs corresponding sham; †*P*<0.01 vs corresponding WT; ‡*P*<0.01 vs corresponding day 3.

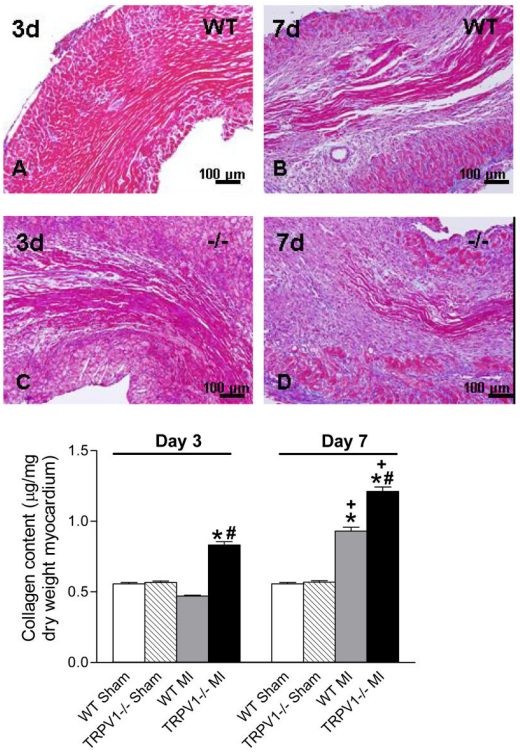

Figure 9.

Collagen deposition in the peri-infarct zone. Upper panel: Masson's trichrome staining for collagen in the infarct region (X200, blue-stained). Lower panel: Quantitative collagen in various groups. N=8. **P*<0.01 vs corresponding sham; †*P*<0.05 vs. WT at the same time point; ‡*P*<0.05 vs. corresponding day 3.

Table 1

Echocardiographic Results after MI in WT and TRPV1$^{-/-}$ Mice

Parameters	Sham		3 Days after MI		7 Days after MI	
	WT	TRPV1$^{-/-}$	WT	TRPV1$^{-/-}$	WT	TRPV1$^{-/-}$
n	16	16	9	8	8	8
Body weight	27.4 ± 0.5	27.9 ± 0.6	27.3 ± 0.6	27.6 ± 0.7	28.0 ± 0.5	28.2 ± 0.6
HR	397 ± 27	392 ± 29	394 ± 28	387 ± 26	364 ± 29	396 ± 30
PWthd, (mm)	0.72 ± 0.06	0.73 ± 0.05	0.78 ± 0.07	0.82 ± 0.08*	0.87 ± 0.09*	0.98 ± 0.07*†‡
PWths, (mm)	1.31± 0.05	1.34 ± 0.07	1.40 ± 0.12	1.49 ± 0.15*	1.70 ± 0.11*‡	1.92 ± 0.12*†‡
LVIDd, (mm)	3.1 ± 0.17	3.2 ± 0.18	4.02 ± 0.26*	4.75 ± 0.29*†	4.52 ± 0.25*‡	5.2 ± 0.28*†‡
LVIDs, (mm)	2.3 ± 0.19	2.4 ± 0.16	2.99 ± 0.28*	4.02 ± 0.25*†	3.76 ± 0.24*‡	4.46 ± 0.27*†‡
% EF	58.5 ± 3.2	57.8 ± 3.4	50.4 ± 3.6*	32.9 ± 3.4*†	42.6 ± 3.8*‡	27.0 ± 3.5*†‡

Data are expressed as mean ± SEM. HR, Heart rate; BW, body weight; PWthd, posterior wall thickness in diastole; PWths, posterior wall thickness in systole; LVIDd, left ventricle internal diameter in diastole; LVIDs, left ventricular internal diameter in systole; EF, left ventricular ejection fraction

$^{*}P<0.05$ vs sham

$^{\dagger}P<0.05$ vs. WT

$^{\ddagger}P<0.05$ vs. corresponding day 3